gravity-induced SU(2)⊗U(1) breaking will be presented elsewhere (R. Arnowitt, A. H. Chamseddine, and P. Nath, to be published).
[15]S. Weinberg, Phys. Rev. Lett. 48, 1303 (1982).
[16]S. Weinberg, in *General Relativity—An Einstein Centenary Survey*, edited by S. W. Hawking and W. Israel (Cambridge Univ. Press, Cambridge, England, 1979), Chap. 16.

Quasifree $(e,e'p)$ Reaction on ^{3}He

E. Jans
National Institute for Nuclear and High Energy Physics (formerly IKO), Amsterdam, The Netherlands

and

P. Barreau, M. Bernheim, J. M. Finn,[a] J. Morgenstern, J. Mougey,[b]
D. Tarnowski, and S. Turck-Chieze
Département de Physique Nucléaire et Hautes Energies, Centre d'Etudes Nucléaires de Saclay, F-91191 Gif-sur-Yvette Cédex, France

and

S. Frullani and F. Garibaldi
Istituto Superiore di Sanità, Laboratorio delle Radiazioni, and Istituto Nazionale di Fisica Nucleare, Sezione Sanità, Roma, Italy

and

G. P. Capitani and E. de Sanctis
Laboratori Nazionali di Frascati, Istituto Nazionale di Fisica Nucleare, 00044 Frascati, Roma, Italy

and

M. K. Brussel
University of Illinois, Urbana, Illinois 61801

and

I. Sick
University of Basel, Basel, Switzerland

(Received 19 April 1982)

The proton momentum distribution of ^{3}He has been determined up to momenta of 310 MeV/c by use of the reaction ^{3}He$(e,e'p)$. The experimental missing-energy resolution, $\delta E_m = 1.2$ MeV, was sufficient to separate the two- and three-body breakup channels. Results for the three-body disintegration have been obtained up to missing-energy values of 80 MeV. The resulting spectral function is compared to the predictions of Faddeev and variational calculations.

PACS numbers: 25.30.Cg, 24.10.-k, 21.40.+d, 25.10.+s

The theoretical progress made in the last decade in the field of nucleon-nucleon interactions and in the calculation of properties of the three-nucleon system with realistic NN forces[1,2] has motivated detailed experimental investigations of such systems. Proton knockout coincidence experiments induced by electrons, performed in the region of quasifree kinematics, allow a direct determination of the proton momentum distribution[3] and can therefore serve as a particularly stringent test of NN interaction models.

In the plane-wave impulse approximation (PWIA) the quasifree scattering process is described as follows: An incident electron is scattered elastically from a moving bound target proton with momentum $\vec{p}$, which is ejected and propagates

as a free proton. The residual two-nucleon system (total energy d_0') is assumed to behave as a spectator and to recoil. Momentum and energy conservation then lead to the invariant quantity, the missing energy $E_m = [(d_0')^2 - \vec{p}^2]^{1/2} + M_p - M_3$ in which M_p denotes the proton rest mass and M_3 the ^{3}He rest mass (for notations, see Ref. 4).

In PWIA one can separate kinematic factors from the nuclear structure information by factorizing the coincidence cross section[5]:

$$\frac{d^6\sigma}{de'\,dp'\,d\Omega_{e'}\,d\Omega_{p'}} = C\left(\frac{d\sigma}{d\Omega}\right)_{ep} S(E_m, \vec{p}). \quad (1)$$

Here C denotes a kinematic factor, $(d\sigma/d\Omega)_{ep}$ represents the off-shell electron-proton cross section, and $S(E_m, \vec{p})$ is the spectral function, defined as the joint probability of finding a proton with momentum $\vec{p}$ in the nucleus and corresponding missing energy E_m. In order to map out the spectral function over a sufficiently wide range in E_m and $\vec{p}$, data were taken under two different kinematic conditions.

The experiment was performed using the 600-MeV linear accelerator of Saclay and the two-spectrometer setup of the HE1 end station.[6] A 0.209-g/cm^2-thick liquid ^{3}He target was used. For a defocussed beam spot (4×6 mm^2) the effective target thickness decreased linearly with the intensity of the beam with a slope of $-12\%/\mu$A. Beam currents up to 1.5 μA were used.

The product of the target thickness, the absolute value of the solid angles, and the detection efficiency of each arm of the apparatus was determined by comparison of the elastic electron scattering cross section, measured periodically at 40° and 52° in both spectrometers, with phase-shift calculations using ground-state charge and magnetic-moment distribution parameters determined at Stanford Linear Accelerator Center and Massachusetts Institute of Technology.[7,8] These elastic measurements were coherent within each run, but a 10% difference was found between the two runs. We took the average of them for the absolute normalization of our results and associated a 5% error bar to this normalization. Additional errors of 4% for the target thickness and of 4% for the effective solid angles were taken into account. Therefore a systematic error of 8% has been added quadratically to the statistical error for each measurement to account for the estimated uncertainty in the absolute normalization.

The true-to-accidental ratio for coincidences varied from 20 to 0.20, depending on the kinematic conditions. The phase-space acceptance volumes and the distribution of the accidental events in the $(E_m, \vec{p})$ plane were determined by means of a Monte Carlo simulation.[9] The data were unfolded and corrected for radiative effects by use of standard formulas[10] which take energy losses due to bremsstrahlung and ionization into account.

The data of Fig. 1 show that the missing-energy resolution of 1.2 MeV was sufficient to separate the (pd) two-body breakup centered at $E_m = 5.5$ MeV, from the (ppn) continuum starting at $E_m = 7.7$ MeV. In order to separate the contribution of the two-body breakup tail from this continuum in the overlap region around 7 MeV, Gaussian shapes were fitted to the data from $E_m = 4.0$ to 6.75 MeV, the resulting curve being also shown in Fig. 1.

The differential cross sections for the reaction ^{3}He$(e, e'p)d$ are listed in Table I as a function of the proton angle $\Theta_{p'}$. The proton scattering angle and the differential cross sections were corrected such that they correspond with coplanar kinematics, the correction factor, calculated in PWIA, being $\leq 3\%$.

The nuclear structure information was obtained from the data by use of the factorized expression (1) for the cross section. The product of the first two terms of Eq. (1) was approximated by the usual formula of the Saclay $(e, e'p)$ experiments.[4,9]

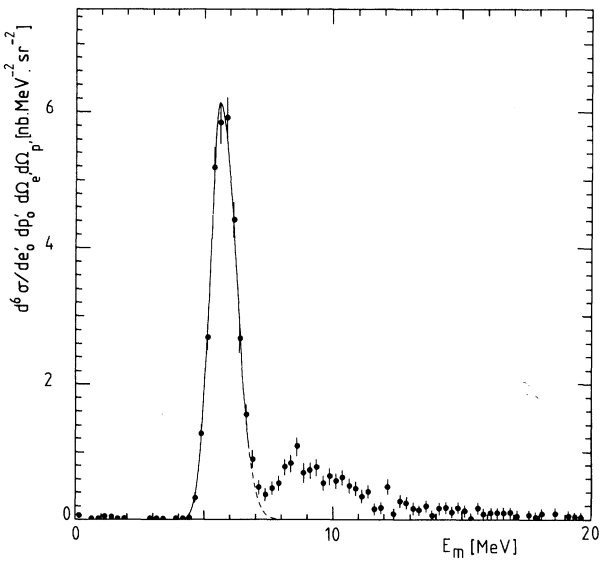

FIG. 1. Radiatively corrected coincidence cross section as a function of missing energy, E_m, measured in kinematics I at $\Theta_{p'} = 64.4°$. The peak at 5.5 MeV corresponds to the two-body breakup channel ^{3}He$(e, e'p)d$.

TABLE I. Fivefold differential cross section for the coplanar reaction ^{3}He$(e,e'p)d$, as a function of the proton scattering angle, Θ_p' (see text). The central value of the detected proton momentum is denoted by $|\vec{p}'|_{cent}$. The errors represent the statistical error only. For kinematics I, e_0 = 527.9 MeV, Θ_e = 52.2°, $|\vec{q}| \simeq 430$ MeV/c; for kinematics II, e_0 = 509.3 MeV, Θ_e = 36.0°, $|\vec{p}| \simeq 300$ MeV/c.

Kinematics I			Kinematics II		
Θ_p'	$\lvert\vec{p}'\rvert_{cent}$ (MeV/c)	$d^5\sigma/de'\,d\Omega_{e'}\,d\Omega_{p'}$ (nb MeV^{-1} sr^{-2})	Θ_p'	$\lvert\vec{p}'\rvert_{cent}$ (MeV/c)	$d^5\sigma/de'\,d\Omega_{e'}\,d\Omega_{p'}$ (nb MeV^{-1} sr^{-2})
53.8	431.6	57.6 ± 1.8	55.4	461.0	2.60 ± 0.14
57.8	431.0	33.8 ± 1.0	68.3	454.5	1.30 ± 0.08
61.7	431.3	16.2 ± 0.4	76.6	446.9	0.629 ± 0.056
65.7	428.5	6.25 ± 0.17	84.1	438.1	0.239 ± 0.022
69.8	424.4	2.55 ± 0.08	92.1	428.1	0.098 ± 0.011
74.0	419.1	0.926 ± 0.043			
77.0	412.6	0.366 ± 0.027			

Integration of the spectral function over a specific missing-energy band results in the proton momentum distribution, $\rho(\vec{p})$, of the selected physical process.

Integration of the two-body breakup peak, centered at 5.5 MeV, gives the proton momentum distribution, ρ_2, corresponding to the residual (pn) pair in the $T=0$ deuteron ground state. Integration of the

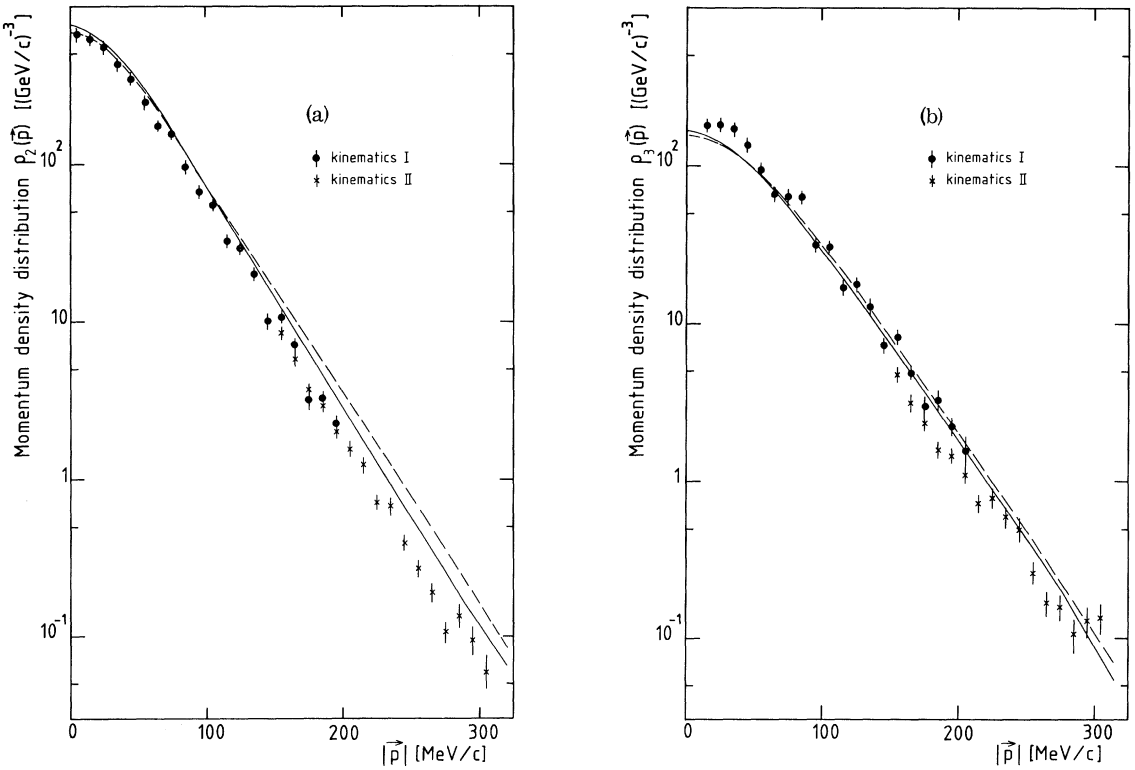

FIG. 2. Proton momentum distribution of ^{3}He for (a) two-body and (b) three-body breakup. The three-body breakup contribution has been obtained by integration up to a missing energy of 20 MeV. Dots and crosses correspond to measurements in kinematics I and II, respectively. The solid curves represent the calculation of Dieperink *et al.* (Ref. 11), the dashed lines that of Ciofi degli Atti, Pace, and Salmè (Ref. 1). The error bars include both the statistical error and an 8% error due to the estimated uncertainty in the absolute normalization.

TABLE II. Proton momentum distributions, ρ_2 and ρ_3, for the two- and three-body disintegrations, respectively. ρ_3 has been obtained by integration of the three-body breakup contribution up to 20 MeV. The errors represent the statistical error only.

$\vec{p}$ (MeV/c)	ρ_2 Kin.I $(\text{GeV/c})^{-3}$	ρ_3 Kin.I $(\text{GeV/c})^{-3}$	$\vec{p}$ (MeV/c)	ρ_2 Kin.II $(\text{GeV/c})^{-3}$	ρ_3 Kin.II $(\text{GeV/c})^{-3}$
5	659 ± 37		155	8.66 ± 0.45	4.76 ± 0.39
15	608 ± 18	180 ±10	165	5.81 ± 0.29	3.14 ± 0.26
25	543 ± 16	182 ± 8	175	3.77 ± 0.20	2.35 ± 0.23
35	427 ± 10	173 ± 8	185	3.00 ± 0.14	1.59 ± 0.15
45	345 ± 8	135 ± 4	195	2.01 ± 0.12	1.47 ± 0.13
55	242 ± 8	94.9 ± 4.2	205	1.58 ± 0.10	1.10 ± 0.11
65	174 ± 4	66.3 ± 2.7	215	1.24 ± 0.11	0.733 ± 0.096
75	156 ± 4	63.6 ± 2.1	225	0.716 ± 0.059	0.787 ± 0.083
85	96.0 ± 3.3	63.4 ± 2.5	235	0.678 ± 0.072	0.598 ± 0.083
95	67.6 ± 1.5	31.5 ± 1.4	245	0.397 ± 0.031	0.492 ± 0.081
105	55.2 ± 1.5	30.7 ± 1.2	255	0.276 ± 0.026	0.260 ± 0.040
115	32.5 ± 1.1	16.9 ± 1.1	265	0.192 ± 0.023	0.167 ± 0.029
125	29.6 ± 0.7	17.9 ± 0.8	275	0.107 ± 0.014	0.160 ± 0.027
135	20.1 ± 0.6	12.8 ± 0.5	285	0.138 ± 0.023	0.108 ± 0.022
145	10.1 ± 0.5	7.25 ± 0.58	295	0.095 ± 0.018	0.130 ± 0.025
155	10.8 ± 0.4	8.25 ± 0.58	305	0.059 ± 0.015	0.134 ± 0.028
165	7.10± 0.33	4.93 ± 0.33			
175	3.14± 0.33	2.97 ± 0.38			
185	3.31± 0.23	3.23 ± 0.37			
195	2.25± 0.23	2.21 ± 0.26			
205		1.56 ± 0.37			

continuum up to 20 MeV gives the proton momentum distribution, ρ_3, corresponding to low-energy unbound states of the $(p+n)$ pair. The two- and three-body breakup momentum distributions for the two kinematics are listed in Table II and plotted in Fig. 2. The full curves correspond to the momentum distributions obtained by integrating the theoretical spectral function calculated by Dieperink *et al.*[11] These authors used the three-body ground-state wave function of Brandenburg, Kim, and Tubis[2] obtained with the Faddeev technique for the Reid soft-core potential interacting in $^1S_0$ and $^3S_1$-$^3D_1$ states. The dashed curves represent the results of a calculation performed by Ciofi degli Atti, Pace, and Salmè,[1] using the variational wave function of Nunberg, Prosperi, and Pace,[12] but with a corrected asymptotic falloff of the harmonic-oscillator basis expansion wave function.

The agreement with theory for the two-body breakup channel is fairly good up to 150 MeV/c. However, experimentally fewer high-momentum components are found beyond this point relative to the theory. No such discrepancy is present in the case of the three-body breakup process, when the continuum is integrated up to 20 MeV.

Previous ^{3}He$(e,e'p)$ experiments[13,14] have been hampered by a lack of energy resolution. Integrating up to 11 MeV missing energy shows that our experiment is in reasonable agreement with the two others and this agreement gives us confidence in the absolute scale of the cross sections.

In the overlap region between the kinematic sets I and II [$150 < \vec{p} < 200$ MeV/c, see Fig. 2(a)], we find the ratio of the integrated spectral-function values corresponding to the two-particle disintegration to be $S_{\text{I}}/S_{\text{II}} = 1.14 \pm 0.10$, in which the error is the quadratic sum of the statistical error and the supplementary error of 8%. Whether this deviation from unity is due to an incorrect off-shell extrapolation of the electron-proton cross section, to the presence of final-state interactions, or to more complicated processes is not clear. Using the ground-state wave function of Brandenburg, Kim, and Tubis,[2] and including meson exchange currents and final-state interactions, Laget[15] improves, especially for the high-momentum components, the agreement

with the experimental two-body breakup momentum distribution. To investigate this deviation from unity in more detail, a full Faddeev calculation of the coincidence cross section in the kinematics of the present experiment is needed for both the two- and three-body breakup.

New and accurate ^{3}He$(e,e'p)$ data have been presented here which may serve as a testing ground for NN potential properties via the calculation of proton momentum distributions in the three-nucleon system. Tables containing the experimental spectral function values in the region $0<E_m<80$ MeV and $0<\vec{p}<310$ MeV/c are available on request.

This work was supported in part by the Dutch Foundation for Fundamental Research on Matter (FOM) and the Swiss National Science Foundation.

[a]Present address: Laboratory for Nuclear Sciences, Massachusetts Institute of Technology, Cambridge, Mass. 02139.

[b]Present address: DRF/CPN, Centre d'Etudes Nucléaires Grenoble, 85X, 38041 Grenoble Cédex, France.

[1]C. Ciofi degli Atti, E. Pace, and G. Salmè, in Proceedings of the Mini-Conference on the Study of Few-Body Systems with Electromagnetic Probes, Amsterdam, November 1981 (unpublished), and private communication.

[2]R. A. Brandenburg, Y. E. Kim, and A. Tubis, Phys. Rev. C 12, 1368 (1975).

[3]G. Jacob and Th. A. J. Maris, Rev. Mod. Phys. 38, 121 (1966).

[4]M. Bernheim *et al.*, Nucl. Phys. A365, 349 (1981).

[5]I. S. Shapiro, V. M. Kolybasov, and G. R. Augst, Nucl. Phys. 61, 353 (1965).

[6]P. Leconte *et al.*, Nucl. Instrum. Methods 169, 401 (1980).

[7]J. S. McCarthy, I. Sick, and R. R. Whitney, Phys. Rev. C 15, 1396 (1977).

[8]P. Dunn, to be published, and thesis, Massachusetts Institute of Technology (unpublished).

[9]J. Mougey *et al.*, Nucl. Phys. A262, 461 (1976).

[10]L. W. Mo and Y. S. Tsai, Rev. Mod. Phys. 41, 200 (1969); Y. S. Tsai, Stanford Linear Accelerator Center Report No. 848, 1971 (unpublished).

[11]A. E. L. Dieperink *et al.*, Phys. Lett. 63B, 261 (1976).

[12]P. Nunberg, D. Prosperi, and E. Pace, Nucl. Phys. A285, 58 (1977).

[13]A. Johansson, Phys. Rev. 136, B1030 (1964); B. F. Gibson and G. B. West, Nucl. Phys. B1, 349 (1967).

[14]I. V. Kozlovsky *et al.*, Nucl. Phys. A368, 493 (1981).

[15]J. M. Laget, private communication.

Is the Shell-Model Concept Relevant for the Nuclear Interior?

J. M. Cavedon, B. Frois, D. Goutte, M. Huet, Ph. Leconte, C. N. Papanicolas,[a]
X.-H. Phan, S. K. Platchkov, and S. Williamson

Département de Physique Nucléaire à Haute Energie, Centre d'Etudes Nucléaires de Saclay, F-91191 Gif-sur-Yvette Cédex, France

and

W. Boeglin and I. Sick

Department of Physics, University of Basel, Basel, Switzerland

(Received 19 July 1982)

The 3s radial wave function $R(r)$ has been determined by electron scattering from ^{206}Pb and ^{205}Tl. The shape of $R(r)$ in the central region of the nucleus is used to test the validity of the independent-particle shell model at large nuclear density.

PACS numbers: 21.65.+f, 21.60.Cs, 25.30.Cg

The shell model was introduced quite late[1] in the historical development of nuclear theory. The strong repulsive core of the nucleon-nucleon interaction, the resulting nucleon-nucleon correlations, and the related saturation of nuclear densities had discouraged the idea of treating nucleons as independent particles moving in an average potential. The success of the shell model came as quite a surprise. The applicability of the shell model is still one of the striking features of finite nuclei.

The foundation of the shell model has been extensively studied since. Nuclear matter theory[2] has enabled us to understand the short healing